Identification of the Catalytically Important Amino Acid Residue Resonances in Ferric Low-Spin Horseradish Peroxidase with Nuclear Overhauser Effect Measurements

V. Thanabal,[1a] Jeffrey S. de Ropp,[1b] and Gerd N. La Mar*[1a]

Contribution from the Department of Chemistry and UCD NMR Facility, University of California, Davis, California 95616. *Received February 17, 1987*

Abstract: Nuclear Overhauser effect (NOE) measurements, saturation transfer spectroscopy, and differential paramagnetic-induced relaxation in conjunction with the available sequence homology with cytochrome *c* peroxidase (CcP) and computer modeling of the heme pocket of horseradish peroxidase (HRP) have led to the location and assignment of the resonances of numerous catalytically important amino acid side chains in the low-spin cyano complex of horseradish peroxidase (HRPCN). Residues identified are the axial His 170, Leu 237, and Tyr 185 on the proximal side and Arg 38, His 42, and Phe 41 on the distal side. NOE connectivities among amino acid side chain protons and between amino acid side chains and previously assigned heme side chain resonances (Thanabal, V.; de Ropp, J. S.; La Mar, G. N. *J. Am. Chem. Soc.* **1987**, *109*, 265-272) place the residues in locations completely consistent with those predicted by the sequence homology to CcP and computer modeling. In particular, the stereochemistry of the proposed catalytically critical residues in the distal pocket, Arg 38 and His 42 (Finzel, B. C.; Poulos, T. L.; Kraut, J. *J. Biol. Chem.* **1984**, *259*, 13027-13036), appears to be highly conserved. The NOE connectivities between known heme side chains and assigned amino acid side chain protons establish that the prosthetic group in deutero-hemin-reconstituted HRPCN is rotated by 180° about the α,γ-meso axis from that in the native enzyme. While the presence of an aromatic side chain (Tyr 185) near the proposed substrate binding site near pyrrole IV is clearly identified by NOE studies, the binding of the substrate near the 8-CH_3 does not significantly alter the orientation of Tyr 185. The potential utility of NOE studies in large paramagnetic enzymes is discussed.

Horseradish peroxidase (HRP) is a single-chain *b*-type hemoprotein that catalyzes the decomposition of H_2O_2 at the expense of aromatic proton donors such as aniline, indole-3-propionic acid (IPA), and benzhydroxamic acid (BHA).[2-4] The absence of X-ray structural data for HRP has placed considerable emphasis on spectroscopic methods,[5-15] sequence homology comparison to structurally characterized cytochrome *c* peroxidase (CcP),[16-20] and computer modeling to obtain information on its active site.[21]

Although the overall homology in the amino acid sequence between CcP[16] and HRP[17] is only 18%, detailed comparison[18] has revealed the apparent conservation of certain residues at both the proximal and distal sides of the heme pocket. An axial (proximal) histidine (His 170 in HRP) is generally accepted as the common binding site of the heme to the polypeptide chain.[22,23] In CcP, important residues in contact with the heme, in addition to the proximal His 175, are Trp 191 and Leu 232 on the proximal side and distal His 52, Arg 48, and Trp 51 on the distal side.[19,20] Poulos and Kraut have proposed[19,20] that the distal His and Arg are key residues in the catalytic mechanism of H_2O_2 decomposition. Trp 51 has been proposed to be the site of the cation radical in formation of the ES complex of CcP.[24] Very recent computer modeling of the HRP heme pocket[21] on the basis of sequence comparison to CcP had led to the proposal that HRP possesses similarly situated distal His and Arg. While Leu 232 (CcP) appears conserved in HRP (Leu 237), the structural homology has Trp 51 in CcP replaced by Phe 41 in HRP over pyrrole II (Figure 1). A tyrosine in the heme pocket of CcP (Tyr 187) appears conserved and the computer model further predicts[21] that Tyr 185 in HRP is in contact with pyrrole IV, which is the region proposed to serve as the binding site for substrate. This Tyr, in fact, has been proposed[21] to be very flexible and move away from the heme in HRP to accommodate the binding of the substrate, BHA.

^{1}H NMR has played a key role in determining structural features of the heme cavity in HRP in all of its functional as well as some nonfunctional states.[8-15] The state for which the NMR methods have been most successfully employed is the low-spin cyano derivative of the resting state enzyme.[10,15] The narrow lines and large magnetic anisotropy[25] lead to a well-resolved ^{1}H NMR spectrum with a large number of resolved resonances arising from both heme and amino acid side chains in the heme pocket. The

(1) (a) Department of Chemistry. (b) UCD NMR Facility.
(2) Dunford, H. B. *Adv. Inorg. Biochem.* **1982**, *4*, 41-68.
(3) Dunford, H. B.; Stillman, J. S. *Coord. Chem. Rev.* **1976**, *19*, 187-251.
(4) Caughey, W. S. In *Inorganic Biochemistry*; Eichorn, G. L., Ed.; Elsevier Scientific Publishing Co.: Amsterdam, 1973; Vol. 2, Chapter 24.
(5) Colvin, J. T.; Rutter, R.; Stapleton, H. J.; Hager, L. P. *Biophys. J.* **1983**, *41*, 105-108.
(6) Nozawa, T.; Kobayaski, N.; Hatano, M.; Ueda, M.; Sogami, M. *Biochim. Biophys. Acta* **1980**, *626*, 282-290.
(7) Callahan, P. M.; Bobcock, G. T. *Biochemistry* **1981**, *20*, 952-958.
(8) La Mar, G. N.; de Ropp, J. S.; Smith, K. M.; Langry, K. C. *J. Biol. Chem.* **1980**, *225*, 6646-6652.
(9) La Mar, G. N.; de Ropp, J. S.; Smith, K. M.; Langry, K. C. *J. Biol. Chem.* **1981**, *256*, 237-243.
(10) de Ropp, J. S.; La Mar, G. N.; Smith, K. M.; Langry, K. C. *J. Am Chem. Soc.* **1984**, *106*, 4438-4444.
(11) La Mar, G. N.; de Ropp, J. S. *J. Am. Chem. Soc.* **1982**, *104*, 5203-5206.
(12) Morishima, I.; Ogawa, S.; Inubushi, T.; Yonezawa, T.; Iizuka, T. *Biochemistry* **1977**, *16*, 5109-5115.
(13) Williams, R. J. P.; Wright, P. E.; Mazza, G.; Ricard, J. R. *Biochim. Biophys. Acta* **1975**, *581*, 127-147.
(14) Thanabal, V.; de Ropp, J. S.; La Mar, G. N. *J. Am. Chem. Soc.* **1986**, *108*, 4244-4245.
(15) Thanabal, V.; de Ropp, J. S.; La Mar, G. N. *J. Am. Chem. Soc.* **1987**, *109*, 265-272.
(16) Takio, K.; Titani, K.; Ericsson, L. H.; Yonetani, T. *Arch. Biochem. Biophys.* **1980**, *203*, 615-629.
(17) Welinder, K. G. *Eur. J. Biochem.* **1979**, *96*, 483-502.
(18) Welinder, K. G. *Eur. J. Biochem.* **1985**, *151*, 497-504.
(19) Poulos, T. L.; Kraut, J. *J. Biol. Chem.* **1980**, *255*, 8199-8205.
(20) Finzel, B. C.; Poulos, T. L.; Kraut, J. *J. Biol. Chem.* **1984**, *259*, 13027-13036.
(21) Sakurada, J.; Takahashi, S.; Hosoya, T. *J. Biol. Chem.* **1986**, *261*, 9657-9662.
(22) Yonetani, T.; Yamamoto, H.; Erman, J. E.; Leigh, J. S. Jr.; Reed, G. H. *J. Biol. Chem.* **1972**, *247*, 2447-2455.
(23) La Mar, G. N.; de Ropp, J. S. *Biochem. Biophys. Res. Commun.* **1979**, *90*, 36-41.
(24) Poulos, T. L.; Freer, S. T.; Alden, R. A.; Xuong, N. H.; Edwards, S. L.; Hamlin, R. C.; Kraut, J. *J. Biol. Chem.* **1978**, *253*, 3730-3735.
(25) Blumberg, W. E.; Peisach, J.; Wittenberg, B. A.; Wittenberg, J. B. *J. Biol. Chem.* **1968**, *43*, 1854-1862.

0002-7863/87/1509-7516$01.50/0 © 1987 American Chemical Society

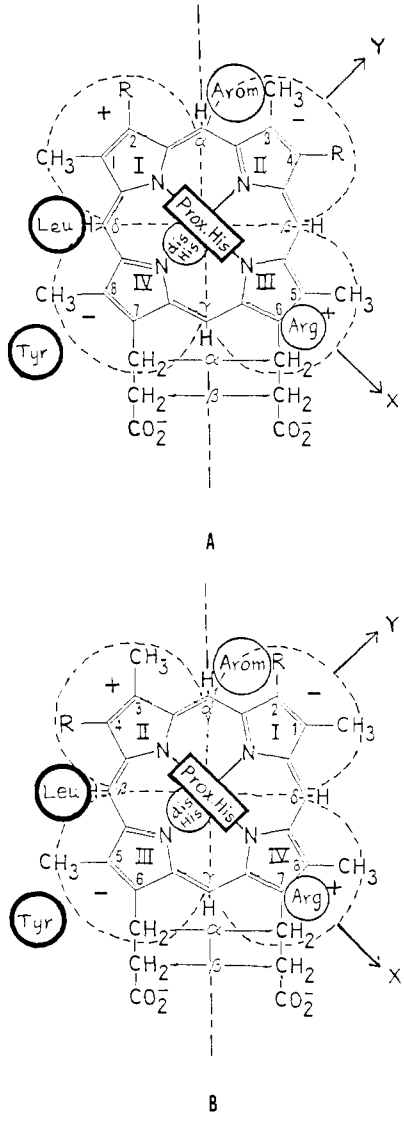

Figure 1. Structure and numbering system for protohemin (R = vinyl) and deuterohemin (R = H) in HRPCN. The in-plane magnetic axes pass through pyrrole nitrogens, as shown.[15] The orientation of the proximal histidyl imidazole plane is shown by a rectangle.[20] The rhombic magnetic anisotropy yields a cloverleaf shaped distribution of dipolar shifts with the lobes alternating in sign with upfield (+) and downfield (−) shifts indicated by the sign of lobes.[15] The location of the functionally relevant amino acid side chains in the heme cavity, as derived from the *Cc*P structure,[20] is shown by circles, with the lighter circle representing the distal side and the darker circle denoting the proximal side. The sequence numbering of the conserved amino acid residues is given with *Cc*P[16] followed by HRP,[17] Arg 48 → Arg 38, distal His 52 → His 42, proximal His 175 → His 170, Tyr 187 → Tyr 185, and Leu 232 → Leu 237. The circle marked Arom indicates an aromatic residue that is Trp 51 in *Cc*P and Phe 41 in HRP. The orientation of the hemin as seen in native HRPCN[10] is depicted in trace A, while trace B represents a 180° rotation of the hemin about its α,γ-meso axis; this latter orientation has been proposed for deuterohemin-HRPCN.[37] Note that the relative positions of the amino acid residues in both trace A and trace B are the same while the pyrroles interchange environments, I ↔ II and III ↔ IV.

necessarily dipolar shifts for the amino acid side chain residues[26,27] could, in principle, yield structural information if the resonances could be assigned unambiguously, the magnetic anisotropy determined, and the magnetic axes located.[28] We have shown[15] that a combination of NMR methods, including analysis of differential paramagnetic relaxation, isotope labeling of the heme, nuclear Overhauser effect measurements, and saturation-transfer from the high-spin resting state HRP, lead to the unambiguous assignment of all 22 heme resonances in HRPCN. Moreover, the pattern of meso-H dipolar shifts indicates[15] that the in-plane magnetic axes pass through pyrrole nitrogens, with magnetic anisotropy that induces rhombic dipolar shifts as described by the cloverleaf pattern depicted in Figure 1. This information on the pattern of dipolar shifts provides key information as to the likely regions of the NMR spectrum that some of the functionally relevant amino acid residues will appear. Thus side chains over pyrroles I and III are expected to yield resonances upfield of their diamagnetic positions and are the likely candidates for numerous non-heme resonances in the upfield portion of the ^{1}H NMR spectrum of HRPCN.[15]

We are interested here in extending the assignments in HRPCN to the non-heme hyperfine shifted resonances, the location of the resonances for functionally relevant side chains, and the determination as to the extent of similarity of the stereochemistry of the heme pocket in HRP to that of *Cc*P[19,20] and to the computer model of HRP.[21] In a general sense we wish to assess the utility of the presently available NMR methodology for elucidating the structure of the heme cavity of large molecular weight paramagnetic heme enzymes. While there is probably an insufficient number of amino acid signals resolved in HRPCN to allow identification of complete spin systems that could lead to unambiguous assignment of amino acid side chains, the residues in close contact with specific portions of the heme periphery can be identified as aromatic or aliphatic on the basis of a large NOE and the location of the intercept at infinite temperature of the hyperfine shift.[26,27,29]

We have already shown[15] that cyanide exchange is sufficiently fast so as to allow saturation transfer from the high-spin ferric resting state of HRP to the low-spin HRPCN complex. Thus all HRP assignments,[8,14,30] such as the proximal histidyl β-CH_2, can be transferred to HRPCN. For nonbonded amino acid side chains, we turn to the nuclear Overhauser effect (NOE),[31] which has been demonstrated to be highly useful in paramagnetic molecules.[14,15,32-34] A summary of the relevant equations and limitations has been presented previously.[15] We utilize here primarily the steady state NOE, which, for short irradiation time, yields an effect that is qualitatively a measure of the inverse sixth power of the distance between the saturated and detected protons.[35] Because of the complexity of the system and the different experimental methods utilized for NOE studies in ^2H_2O and H_2O solution,[36] we focus here solely on the non-exchangeable signals detected in the former solvent.

Experimental Section

Horseradish peroxidase (HRP), type VI, was purchased from Sigma as a lyophilized, salt-free powder and used directly without further purification; the protein is predominantly isozyme C. HRPCN complexes reconstituted with 1,5-$(C^2H_3)_2$-hemin and deuterohemin used in this study are the same as those reported earlier.[10,37] Solutions for proton

(26) Satterlee, J. D. *Annu. Rep. NMR Spectrosc.* **1986**, *17*, 79–178.
(27) La Mar, G. N. In *Biological Application of Magnetic Resonance*; Shulman, R. G., Ed.; Academic: New York, 1979; pp 305–343.
(28) Williams, G.; Moore, G. R.; Porteous, R.; Robinson, M. N.; Soffe, N.; Williams, R. J. P. *J. Mol. Biol.* **1985**, *183*, 409–428.
(29) Jesson, J. P. In *NMR of Paramagnetic Molecules*; La Mar, G. N., Horrocks, W. D., Jr., Holm, R. H., Eds.; Academic: New York, 1973; pp 1–51.
(30) Thanabal, V.; de Ropp, J. S.; La Mar, G. N., manuscript in preparation.
(31) Noggle, J. H.; Shirmer, R. E. *The Nuclear Overhauser Effect*; Academic: New York, 1971.
(32) Ramaprasad, S.; Johnson, R. D.; La Mar, G. N. *J. Am. Chem. Soc.* **1984**, *106*, 5330–5335.
(33) Unger, S. W.; Lecomte, J. T. J.; La Mar, G. N. *J. Magn. Reson.* **1985**, *64*, 521–526.
(34) Trewhella, J.; Wright, P. E.; Appleby, C. A. *Nature (London)* **1980**, *280*, 87–88.
(35) Dobson, C. M.; Olejniczak, E.; Poulsen, F. M; Ratcliffe, G. *J. Magn. Reson.* **1982**, *48*, 97–110.
(36) In H_2O, the use of a 1–3–3–1 or Redfield pulse sequence gives a narrow window of excitation and it is not possible to excite all the resonances evenly in the spectrum of HRPCN. This leads to the situation that more than one experiment is necessary to obtain the NOE connectivities from a single peak.
(37) La Mar, G. N.; de Ropp, J. S.; Smith, K. M.; Langry, K. C. *J. Am. Chem. Soc.* **1980**, *102*, 4833–4835.

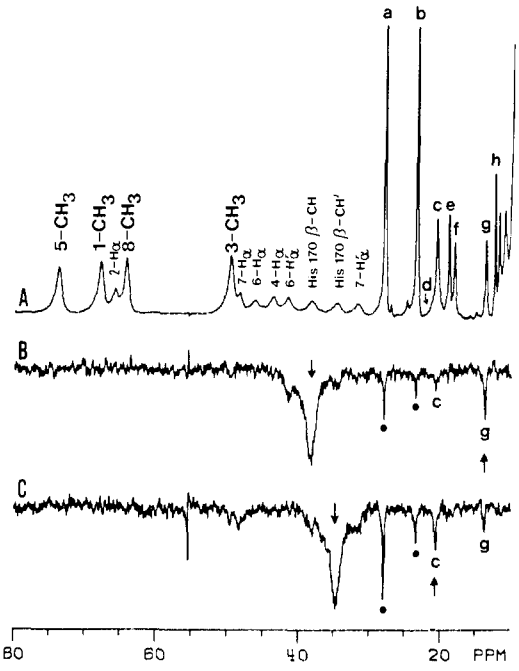

Figure 2. The low-field hyperfine shifted portion of the 360-MHz ^1H NMR spectrum of (A) a mixture of HRP and HRPCN in the ratio 35:65 in 100% ^2H_2O at 55 °C, pH 7.0. Previously assigned HRP resonances[8,30] are labeled. Traces B and C are the saturation-transfer difference spectra generated by subtracting the reference spectrum with the decoupler off-resonance from a similar spectrum of the same sample in which the desired resonance in HRP was saturated. In each of the difference spectra B and C, a downward arrow indicates the peak being saturated and an upward arrow indicates saturation transfer. A filled circle denotes off-resonance power spillage. Trace B shows saturation-transfer to peak g while trace C shows that to peak c. The appearance of peak c in trace B and peak g in trace C is due to a large NOE between peaks c and g in HRPCN (see text).

NMR studies were 3 mM in protein in nominal 100% ^2H_2O. The solution pH, adjusted with 0.2 M ^2HCl or 0.2 M NaO^2H, was measured with a Beckman Model 3550 pH meter equipped with an Ingold microcombination electrode; pH values are not corrected for the isotope effect. Excess solid KCN was added to the protein to generate solutions of HRPCN. For the experiments utilizing a mixture of HRP/HRPCN as described below, the appropriate fractional equivalent of cyanide was added in ^2H_2O. Typically a mixture of HRP/HRPCN in the ratio 35:65 was used for saturation transfer experiments. A 50 mM solution of benzhydroxamic acid (BHA) in ^2H_2O was titrated into a 3 mM HRPCN solution to generate the desired HRPCN:BHA complex.

The buildup of the NOE is time dependent and for an isolated two-spin system it takes the form[31]

$$\eta_i(t) = \frac{\sigma_{ij}}{\rho_i}(1 - e^{-\rho_i t}) \quad (1)$$

where $\rho_i^{-1} = T_{1i}$, the selective spin-lattice relaxation time of H_i, t is the duration of the saturating pulse on H_j, and σ_{ij}, the cross-relaxation between H_i and H_j, is given by[31]

$$\sigma_{ij} = \frac{-\hbar^2\gamma^4}{10r_{ij}^6}\tau_c \quad (2)$$

where τ_c is the reorientation time of the vector defined by H_i and H_j, and r_{ij} is the length of this vector. For short irradiation times (<30 ms) η_i takes the form

$$\eta_i(t) = \sigma_{ij}t \quad (3)$$

and is independent of the T_1 of the nucleus.

NOE and saturation transfer measurements were performed on Nicolet NM-500 and NT-360 FT NMR spectrometers, respectively. The data were collected and analyzed as described earlier.[15] Signal to noise was improved by exponential apodization which introduced 10–30 Hz line broadening. Peak shifts were referenced to the residual water signal which in turn was calibrated against internal 2,2-dimethyl-2-silapentane-5-sulfonate, DSS. Chemical shifts are reported in parts per million (ppm) with downfield shifts taken as positive. Nonselective T_1s were

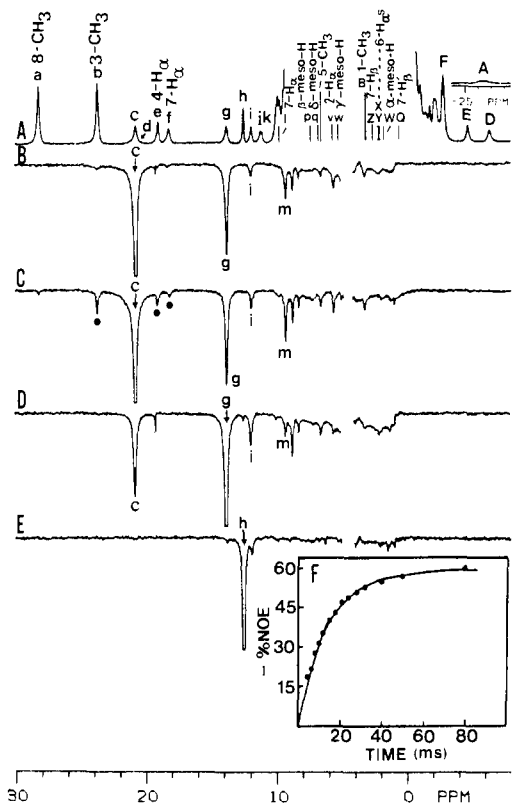

Figure 3. 500-MHz ^1H NMR spectrum of (A) 3 mM HRPCN in 100% ^2H_2O at 55 °C, pH 7.0. Previously assigned peaks are labeled.[10,15] The previously assigned heme resonances in the 0–10-ppm region are shown as a stick diagram. Traces B to E are the NOE difference spectra obtained upon saturating the resonance marked by an arrow; filled circles denote effects due to power spillage. Trace B shows saturation of peaks c and d with low power, while Trace C shows saturation with high power (see text). Note the strong NOE to peak g. The signal m shows a large intensity change in going from trace B to trace C. Trace D: saturate the peak g; note the strong reciprocal NOE to the peak c. Trace E: saturate the signal h; note the absence of detectable NOEs. Trace F: plot of time-dependent buildup of the NOE to the geminal partner g following the presaturation of the peak c for varying times, t, from 4 to 80 ms. The solid line represents a fit of the data with eq 1, which yields $\sigma_{(c\rightarrow g)} = -39$ Hz and $\rho_{(g)} = 66$ Hz.

determined by a variation of the standard inversion–recovery sequence to include a composite 180° pulse.[38] The T_1 was computed by a non-linear least-squares fit to the equation

$$(I_\infty - I_\tau)/2I_\infty = A\exp(-\tau/T_1) \quad (4)$$

where I_τ and I_∞ are the intensities of the resonance at τ and $>5T_1$, respectively, after the 180° pulse, and τ is the delay, in ms, between the 180° and 90° pulses. The necessarily dipolar paramagnetic relaxation that determines T_1s for a non-coordinated residue dictates that[39,40]

$$r_i/r_j = [T_{1i}/T_{1j}]^{1/6} \quad (5)$$

where i and j are two nonequivalent protons and r is their distance to the paramagnetic center. The distance of a proton from the iron was calculated by using 3-CH_3 (r = 6.1 Å) as reference in the above equation.

Results

The 360-MHz spectrum of a partially cyanide ligated HRP solution in ^2H_2O at 55 °C is illustrated in trace A of Figure 2. The high-spin resting state peaks resonate in the region 40–100 ppm,[8] while those of low-spin HRPCN appear upfield of 40 ppm.[10,15] The assignments for the resting state HRP, deduced

(38) Freeman, R.; Kempsell, S. P.; Levitt, M. H. *J. Magn. Reson.* **1976**, *38*, 453.
(39) Cutnell, J. D.; La Mar, G. N.; Kong, S. B. *J. Am. Chem. Soc.* **1981**, *103*, 3567–3572.
(40) Swift, T. J. In *NMR of Paramagnetic Molecules*; La Mar, G. N., Horrocks, W. D., Jr., Holm, R. H., Eds.; Academic: New York, 1973; pp 53–83.

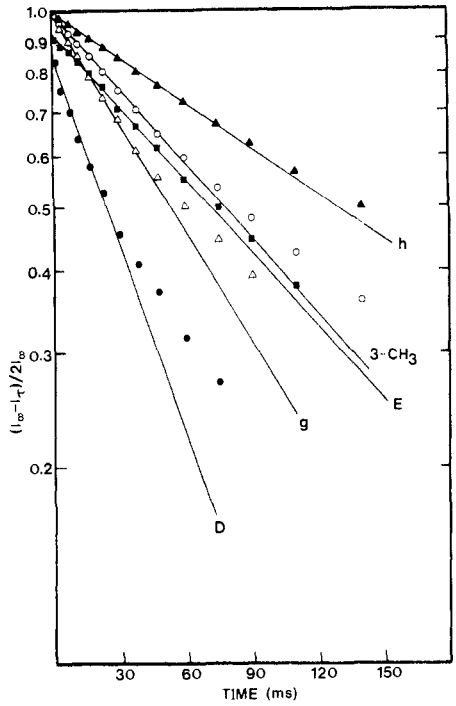

Figure 4. Semilogarithmic plots of normalized intensity, $(I_\infty - T_\tau)/(2I_\infty)$ (eq 4), versus delay time, τ, for a 180°–τ–90° inversion–recovery T_1, determination for peak 3-CH_3, (○), g (△), h (▲), D (●), and E (■) at 55 °C in ^2H_2O, pH 7.0. The solid lines represent the initial slopes which directly yield the T_1 values listed in Table I.

from isotope labeling[8] (all but heme propionate H_αs), NOEs[30] (heme propionate H_αs), and on the basis that only the axial ligand beside the heme can exhibit significant hyperfine shifts for high-spin iron(III) heme[27,30,41] (axial histidine H_βs), are included in the trace. The 500-MHz ^1H NMR spectrum of pure low-spin HRPCN at 55 °C is given in trace A of Figure 3. The expanded upfield portion of the spectrum is shown in trace A of Figure 7. A combination of isotope labeling, saturation transfer from the assigned high-spin HRP spectrum, and NOEs within the low-spin HRPCN complex has yielded the unambiguous location and assignment of all 22 heme resonances,[15] as indicated in Figures 3A and 7A; the positions of the unresolved heme signals are illustrated by a stick diagram. Beside the 22 heme resonances, only the two broad peaks, A and d, have been identified, and these have been assigned[42] to the axial histidine ring 2′-H and 4′-H signals, respectively, on the basis of comparison to model compounds, paramagnetic relaxation effects, and response of their hyperfine shifts to electronic purturbation of heme substituents. Obvious additional resolved nonlabile amino acid resonances are the single-proton peaks c, g, H, I, J, K, D, E, K and N, and the 3-proton peaks M and F.

Nonselective Spin–Lattice Relaxation Times. The results of an inversion–recovery T_1 determination for the resolved amino acid resonances, as well as the reference 3-CH_3 signal, are illustrated in Figure 4. The semilogrithmic plots are linear for only for very short times ($< \sim T_1$), as expected for protons experiencing strong cross relaxation, particularly with slower relaxing protons.[43,44] The initial slope of such a plot, however, still yields a reasonable estimate of the paramagnetic contribution to T_1; such values are listed in Table I. The heme 3-CH_3 signal serves as the reference proton (H_j) in eq 5, with T_1(3-CH_3) = 112 ms and r(3-CH_3···Fe) ~ 6.1 Å. Spectral overlap for several important amino acid peaks (N, M, K, and F) precluded obtaining accurate T_1 values.

Table I. Chemical Shifts and Assignments of Amino Acid Side Chains in HRPCN and Deuterohemin-HRPCN at 55 °C, pH 7.0[a]

peak designation[b]	assignment[c]	HRPCN shift, ppm	HRPCN intercept at T^{-1} = 0, ppm	HRPCN T_1,[d] ms	deutero-hemin-HRPCN[e] shift, ppm
c(1)	His 170 β-CH	20.80	−9.8	80	20.45
d(1)	His 170 4′-H	20.80	−9.8		17.15
g(1)	His 170 β-CH′	13.80	−4.7	80	13.25
h(1)	His 42 2′-H	12.45	3.6	190	12.30
i(1)	*f*	11.85	1.0	100	11.60
j(1)	*f*	11.10	10.0	~10^3	11.10
k(1)	*f*	11.05	10.0	~10^3	11.05
m(1)	His 170 α-CH	9.25	0.0		8.42
n(2 or 3)	Tyr 185 ring H	7.75	7.75		7.78
s(1)	Phe 41 ring H	6.30	8.2		
t(1)	Aromatic	5.75	9.0		5.82
u(1)	Phe 41 ring H	5.55	9.0		
A(1)	His 170 2′-H	−26.30	11.0		−25.10
D(1)	Arg 38 δ-CH	−6.45	0.5	45	−6.50
E(1)	Arg 38 β-CH	−4.75	4.2	90	−4.50
F(3)	Leu 237 δ-CH_3	−2.90	1.3	85[g]	−3.10
K(1)	Arg 38 γ-CH	−1.52	−3.2	15[g]	−1.60
M(3)	*f*	−0.75	0.8		−0.65
N(1)	Arg 38 β-CH′	−0.60	2.3		−0.48
P(3)	Leu 237 δ′-CH_3(?)	0.10	1.3		0.10
R(1)	Arg 38 γ-CH′	0.60	h		0.46
S(1)	Arg 38 α-CH(?)	0.60	3.4		0.46
T(1)	Arg 38 δ-CH′	0.90	1.2		0.82
U(1)	Leu 237 β-CH(?)	1.10	3.5		1.10
V(1)	Leu 237 β-CH′(?)	1.30	3.0		1.30
A′(1)	Leu 237 α-CH(?)	3.00	6.0		3.00

[a] Chemical shift in ppm referenced to DSS through the residual water signal, uncertainty in shifts is ±0.02 ppm. [b] The number of protons giving rise to the resonance is indicated in parantheses. [c] Tentative assignments are marked by a question mark. Heme assignments are given in Table I of ref 15. [d] T_1 values are reported only for the resolved signals; the uncertainty in the values is ±10 ms. [e] The assigned heme resonance positions (in ppm from DSS, 55 °C, pH 7.0) are 5-CH_3 (26.00), 1-CH_3 (21.24), 6-H_α (21.96), 6-H′$_\alpha$ (10.45), 7 H_βs (−1.98), 2-H (−22.54), 4-H (−10.94). [f] Available data do not permit assignment. [g] T_1 values are estimated from the null points. [h] Not determined.

However, the null points,[45] τ_{null}, of the partially relaxed spectra yield reasonable estimates of their T_1s ($T_1 \sim \tau_{null}/\ln 2$), and such values are included in Table I.

Proximal Histidine. Saturation of the two assigned coordinated His 170 H_βs in high-spin HRP leads to saturation transfer exclusively to peaks c,g, as shown in traces B and C of Figure 2. The shorter T_1s of peaks c and g compared to peaks a and b differentiate the saturation transfer from the off-resonance perturbation of peaks a and b. Thus c,g must be the β-methylene

(41) Heistand, R. H.; Lauffer, R. B.; Fikrig, E.; Que, L., Jr. *J. Am. Chem. Soc.* **1982**, *104*, 2789–2796.
(42) La Mar, G. N.; de Ropp, J. S.; Chacko, V. P.; Satterlee, J. D.; Ernian, J. E. *Biochim. Biophys. Acta* **1982**, *708*, 317–325.
(43) Granot, J. *J. Magn. Reson.* **1982**, *49*, 257–270.
(44) Sletten, E.; Jackson, J. T.; Burns, P. D.; La Mar, G. N. *J. Magn. Reson.* **1983**, *52*, 492–496.
(45) Becker, E. D. *High Resolution NMR—Theory and Chemical Applications*; Academic: New York, 1980; Chapter 10.

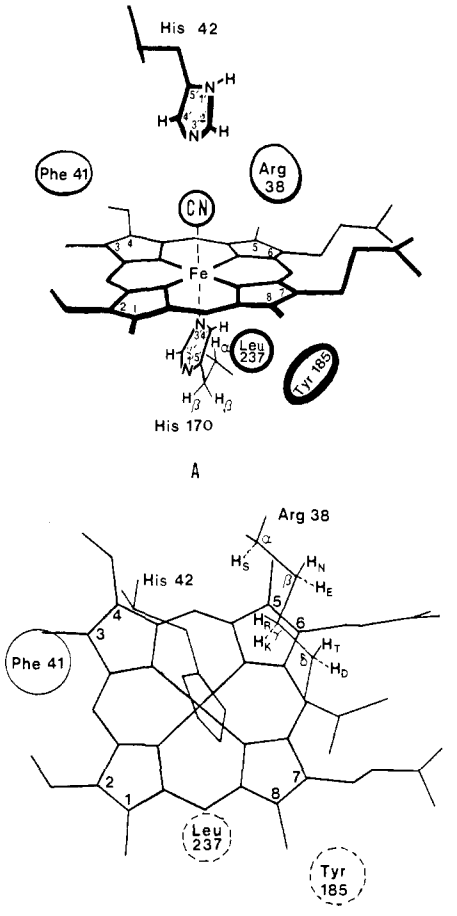

Figure 5. Schematic diagram of the proposed heme pocket of HRPCN.[20,21] Trace A shows edge view with the spatial disposition of amino acid side chains. The darker line represents closer to the viewer while the lighter line is farthest from the viewer. The numbering for protons of the proximal and the distal histidines is also shown. Trace B illustrates the face-on view from the distal side; the amino acid residues on the distal side of the heme are marked by continuous lines, while those on the proximal side are indicated by dashed lines. The individual protons on the Arg 38 residue are also shown with their subscript indicating the labeling of the corresponding resonance in the ^{1}H NMR spectrum of HRPCN (Figure 7).

protons in HRPCN. The geminal nature of peaks c,g is confirmed by NOE studies solely within HRPCN. Saturation of peak c (traces B and C in Figure 3) yields a ~50% NOE to g, as well as to several peaks in the diamagnetic region. The reciprocal NOE from g to c is also observed (Figure 3D). The quantitative use of NOEs and the dominance of primary NOEs at short irradiation times are strongly supported by a study of the time dependence of the NOE between resonances c and g. $\eta(t)$ for peak g upon saturating c is illustrated in the inset F of Figure 3. The solid line represents the computer least-squares fit of the data points to eq 1, which yields $\sigma = -39$ Hz and $\rho = 66$ Hz. Since the β-CH_2 interproton distance is known to be 1.77 Å, eq 2 yields $\tau_c = 21$ ns for the reorientation rate of this interproton vector. This correlation time compares very well with the overall protein tumbling time at 55 °C as obtained from ^{2}H NMR quadrupolar relaxation of deuterium labels on the heme skeleton,[46] or from time-dependent NOE data for an immobile heme propionate group.[15] All subsequent NOE experiments are restricted to a saturation time of 30 ms.

Both peaks c and g exhibit several common NOEs in the region 0–12 ppm, any one of which could be the remaining H_α. Only peak i and the signal m at 9.25 ppm, however, exhibit the strong temperature dependence in the Curie plot expected for the H_α origin (Figure 6), with apparent intercepts near 0 ppm, consistent with primarily dipolar hyperfine shift for such a functional group. The upfield bias of the intercepts could be due to the ring current effect of the heme group. If we assume that the orientation of the proximal His imidazole relative to the polypeptide skeleton is similar in C*c*P[19,20] and HRP, the geometry of the proximal His in C*c*P predicts that H_α is closest to the ring 4′-H (2.0 Å) and hence predicts H_α will exhibit a strong NOE from peak d. Unfortunately, peak d overlaps peak c at all temperatures in HRPCN, precluding selective saturation. However, differentiation between NOEs from peak c and peak d can be made by taking advantage of their very different T_1s and the resulting differential degree of saturation at low radio frequency power. The traces representing low-power saturation and high-power saturation are illustrated in spectra B and C of Figure 3. Only peak m at 9.25 ppm increases dramatically (as compared to the degree of saturation at peak c) in trace C versus trace B, arguing that it originates from H_α and that the stereochemistry of the proximal histidine is indeed very similar to HRP and C*c*P. These conclusions are supported by NOE studies on deuterohemin-HRPCN, where the analogous peaks do not overlap (see below). Thus all of the nonlabile protons of the proximal His 170 have been located and assigned.

The Distal Catalytic Residues. The apparent sequence homology between C*c*P[16] and HRP,[17,18] together with the computer modeling of the HRP heme pocket,[21] indicates the presence of Arg 38 and the distal His 42 as shown in Figure 5. The extended, essentially planar trimethylene side chain of Arg 38 extends over pyrrole III, making contacts with the heme 5-CH_3, 6-β-CH_2, and γ-meso-H. Since in this region the axial dipolar shift is small while the rhombic dipolar shifts are necessarily positive,[15,47] we expect the signals to resonate in the upfield portion of the ^{1}H NMR spectrum.

The relevant upfield portion of the 500-MHz ^{1}H NMR spectrum of HRPCN in ^2H_2O at 55 °C is shown in Figure 7A, with the known heme resonance assignments marked. Irradiation of peak D yields a large (~50%) NOE to a peak at 0.9 ppm designated T, as well as small NOEs (~5–10%) to resolved amino acid peaks E, K, and N and an unresolved peak we designate as R, at 0.6 ppm (Figure 7B); also noteworthy is the large NOE to peak H. Saturation of peak E yields a ~50% NOE to peak N, and weaker NOEs to peaks D, H, and K, a composite R, S at 0.6 ppm, and peak T (0.9 ppm) and peak t at 5.7 ppm (Figure 7C). Saturation of peak K always yields off-resonance saturation effects in the diamagnetic envelope. However, the prominant NOEs to 0.6 ppm, peak R (~50%), as well as smaller NOEs to peaks D, E, and T (Figure 7D), can be distinguished on the basis of variable saturation-power studies. The common interconnectivity of the six peaks D, E, K, N, R, and T, together with ~50% NOEs indicative of geminal methylene pairs for peaks D, T, the resolved peaks E, N, and K, R, point to these six protons as arising from a contiguous trimethylene chain. A planar carbon skeleton for a $(CH_2)_3$ chain leads to interproton distances of 2.5 Å between any pair of protons on the same side of the carbon plane, 1.77 Å between the geminal partners and 3.1 Å between two nonge-

(46) Thanabal, V.; Johnson, R. D.; La Mar, G. N., unpublished results.

(47) The heme hyperfine shifts arise from a combination of the dipolar and contact contribution. The relevant dipolar shift has the form[15,27,29,48]

$$\left(\frac{\Delta H}{H}\right)_{dip} = -\frac{1}{3N}\left[\chi_z - \frac{1}{2}(\chi_x + \chi_y)\right]\frac{3\cos^2\theta - 1}{r^3} - \frac{1}{2N}(\chi_x - \chi_y)\frac{\sin^2\theta\cos 2\Omega}{r^3}$$

where r is the length of the Fe–H vector, θ is the angle between r and the z axis, and Ω is the angle between the projection of r on the heme plane and the x axis; χ_x, χ_y, χ_z are the principle components of the susceptibility tensor in the coordinate system defined in Figure 1. The axial dipolar shift (first term in the equation) is upfield for heme substituents and for amino acid side chains outside the magic angle ($\theta > 54°$) and downfield for those inside the magic angle cone. The relative magnitude of the rhombic geometric factor as a function of Ω yields a cloverleaf distribution as shown in Figure 1. It has been determined that $\chi_y > \chi_x$, so that the rhombic dipolar shift is upfield for amino acid side chains over pyrroles I and III and downfield for those over pyrroles II and IV.

(48) La Mar, G. N.; Walker, F. A. In *The Porphyrins*; Dolphin, D., Ed.; Academic: New York, 1979; Vol. 4, pp 61–157.

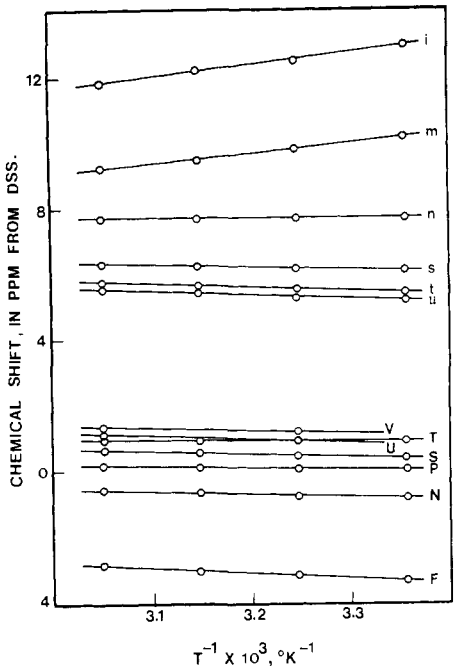

Figure 6. Curie plots of the chemical shifts versus reciprocal temperature of the resonances in the 0–10-ppm region in HRPCN at pH 7.0 located by NOE techniques; the extrapolated diamagnetic intercept at $T^{-1} = 0$ is given in the Table I. The peaks are labeled as shown in Figures 3, 7, and 8 and Table I.

minal protons on opposite sides of the carbon plane. Thus the pattern of three pairs with strong (~50%) NOEs and weak NOEs to all of the other five protons in the fragment is expected. This linear trimethylene fragment can only arise from either a lysine or arginine, and on the basis for a proposed arginine group in the heme pocket[21] it is assigned to Arg 38.

Support for the proposed Arg 38 origin for these resonances, as well as their assignment to individual protons, can be made on the basis of NOE connectivities to previously assigned[15] heme resonances and T_1 values. Thus saturation of peak D yields a strong NOE to peak H, the heme 6-propionate $H_\beta s$ (Figure 7B), while saturating peak E yields an NOE to the heme 5-CH_3 as well as 6-H_β (Figure 7C). The localization of the trimethylene chain over pyrrole III (Figure 5) confirms that it originates from Arg 38, as found for Arg 48 in C*c*P.[20] Peaks analogous to D and E are observed in C*c*PCN.[49] If we assume essentially the same orientation for the distal Arg in HRP as in C*c*P, the NOEs to the heme assign peaks E and N to the β-CH_2, K and R to the γ-CH_2, and D and T to the δ-CH_2, as shown in Figure 5B.

The upfield dipolar shift for these Arg methylene protons is consistent with the prediction of the rhombic anisotropy and the magnetic axis as determined previously.[15,47] The more strongly shifted of these signals, D, E, and K, must arise from the protons closest to the heme plane (Figure 5B), since for these protons both the rhombic as well as the axial dipolar shifts are upfield. Their respective geminal partners, T, N, and R, experience upfield rhombic but downfield axial dipolar shifts,[15,47] and hence they exhibit much smaller hyperfine shifts. The qualitative T_1 values for peaks K, D, and E, 15, 45, and 115 ms, respectively, are qualitatively consistent with their relative distances from the iron, 4.25, 4.40, and 5.74 Å, respectively, as determined for C*c*P[20] (Figure 5B), and further serve to confirm the specific assignments for Arg 38. The strong cross relaxation due to their geminal partners precludes quantitative interpretation of the T_1s in terms of distance. A candidate for the H_α of Arg 38 is a peak at 0.60 ppm (peak S) observed upon saturating both E and K (Figure 7). Variable temperature splits this peak from R, yielding an intercept near 3.0 ppm.

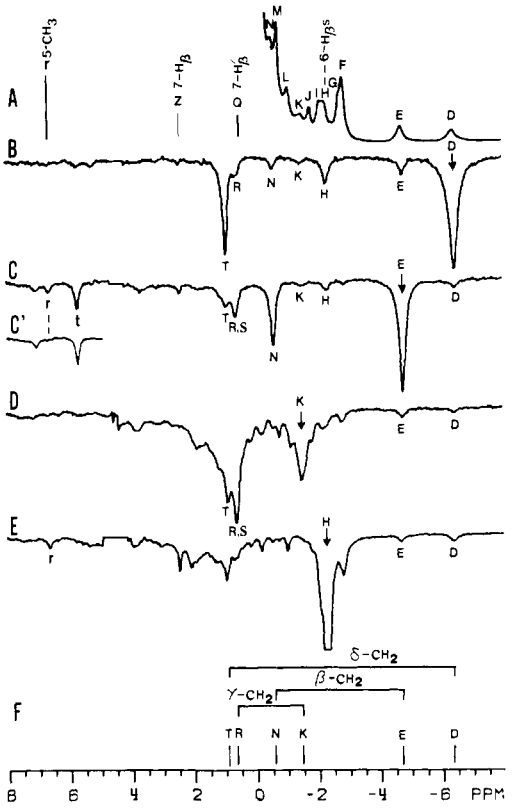

Figure 7. Upfield hyperfine shifted portion of the 500-MHz ^{1}H NMR spectrum of (A) 3 mM HRPCN in 100% ^2H_2O at 55 °C, pH 7.0. The resolved peaks are labeled and unresolved heme peaks are indicated by stick diagram; peaks G, I, J, and L are vinyl H_βs.[10,15] Traces B to E are the NOE difference spectra obtained upon saturating the resonance marked by an arrow. Filled circles denote off-resonance power spillage. Trace B: saturate the resonance D; note the strong NOE to the peak T and weak NOEs to the peaks E, H, K, N, and R. Trace C: saturate the signal E; note the strong NOE to the peak N and the weak NOEs to the peaks D, H, K, T, and *t* and a composite peak R, S (neither R nor S correspond to Q (7-H_βs), as found by variable-temperature studies (not shown)). Also note the weak NOE to the 5-CH_3 resonance *r*. The inset (trace C′) shows the portion of the NOE difference spectrum obtained with HRPCN reconstituted with 1,5-$(C^2H_3)_2$-hemin;[10] note the disappearance of the 5-CH_3 resonance *r*. Trace D: saturate the peak K; note NOEs to peaks D, E, Q, R, and T. Trace E: saturate 6-H_βs resonance H; note NOEs to the peaks D, E, and r (5-CH_3). Part F: stick diagram showing the assignment of the Arg 38 side chain protons.

The peak at 5.7 ppm (peak t) observed when irradiating Arg H_β (peak E) exhibits a variable-temperature intercept at 9.2 ppm (Figure 6; Table I), which indicates a close contact with an aromatic amino acid side chain. Available sequence homology with C*c*P does not allow us to propose an assignment for the residue at this time.

Evidence for the distal His 42 in the ^{1}H NMR spectrum of HRPCN in ^2H_2O is less direct, but nevertheless compelling. The low-field nonlabile proton peak h is narrower (20 Hz) than any other peak, and upon saturation (Figure 3E) it fails to yield a significant detectable NOE to any other non-exchangeable proton. Both the small line width and the absence of dipolar connectivities to other nonlabile protons argue for an origin in the relatively isolated 2′-H of histidine, as is also clearly observed for the distal histidine in sperm whale met-cyano myoglobin.[50] The downfield dipolar shift is completely consistent with the position of 2′-H close to the pseudo-four-fold axis, for which the dominant axial dipolar shift is necessarily downfield.[15,47] The relaxation time of h, ~190 ms, indicates a 6.7-Å distance from the iron, which is also consistent with the 2′-H geometry in C*c*P; again C*c*PCN exhibits a similarly narrow downfield resonance.[49] Further support for this assignment, as well as some details of the hydrogen bonding

(49) Satterlee, J. D.; Erman, J. E.; La Mar, G. N.; Smith, K. M.; Langry, K. C. *J. Am. Chem. Soc.* **1983**, *105*, 2099–2104.

(50) Lecomte, J. T. J.; La Mar, G. N. *Eur. Biophys. J.* **1986**, *13*, 373–381.

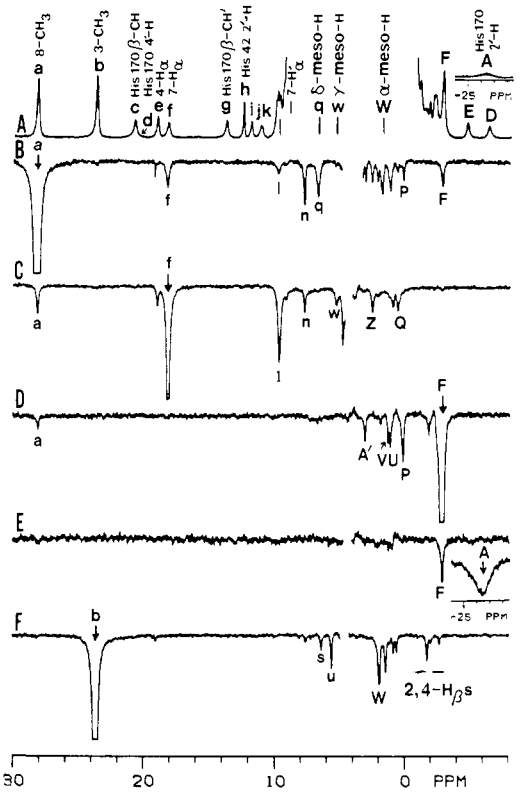

Figure 8. 500-MHz ^{1}H NMR spectrum of (A) 3 mM HRPCN in 100% ^2H_2O at 55 °C, pH 7.0. Previously assigned peaks are labeled.[10,15,37] Traces B to F are the NOE difference spectra obtained by saturating the resonance marked by an arrow; filled circles denote off-resonance power spillage. Trace B: saturate 8-CH_3; note NOEs to the peaks n, q (δ-meso-H).[15] P, and F. Trace C: saturate 7-H_α resonance f; note NOE to the signal n. Trace D: saturate peak F; note the NOEs to the peaks P, U, V, A′ and the 8-CH_3 resonance a. Trace E: saturate His 170 2′-H[42] resonance A; note NOE to the signal F. Trace F: saturation of 3-CH_3 resonance b; note NOEs to the peaks s and u, among others; the NOEs to vinyl H_βs have been discussed previously.[15]

network on the distal side, can be obtained from NOE studies in H_2O solution and will be considered in a subsequent report.

Peripheral Amino Acid Contacts. While most close peripheral amino acid contacts are not conserved in CcP and HRP, certain important homologies exist.[16-18] The important proposed replacements in CcP → HRP are Trp 51 → Phe 41 over pyrrole II on the distal side and Trp 191 → Asn 189 on the proximal side. A group sometimes proposed as functionally important, Leu 232 → Leu 237, over the junction of pyrrole I and IV on the proximal side, and Tyr 187 → Tyr 185 in contact with pyrrole IV, appears conserved.

Saturation of 8-CH_3 (peak a) on pyrrole IV yields sizable NOEs to ~7.75 ppm, (peak n), ~0.1 ppm (peak P), and the upfield three-proton peak, F, as well as δ-meso-H (peak q) (Figure 8B). Saturating 7-H_α (peak f) gives NOEs to the same 7.75 ppm resonances n (Figure 8C); deconvolution of this peak n reveals at least two components (not shown). Variable-temperature data for these resonances indicate essentially temperature-independent shifts (Figure 6), which establish the origin of n as an aromatic side chain with negligible dipolar hyperfine shift which can be attributed to Tyr 185. Irradiating the apparent methyl peak F at low power so as not to significantly excite peak G (4 vinyl $H_{\beta-c}$) yields NOEs to peaks at ~0.1 (P), 1.1 (U), 1.3 (V), and 3.0 (A′) ppm, in addition to a small NOE to 8-CH_3 (Figure 8D). A small NOE to peak F can also be detected when the proximal His 170 2′-H (peak A) is saturated (Figure 8E). Analysis of the CcP structure[20] indicates that the δ-CH_3 of Leu 237 occupies a position consistent with the observed NOE pattern. The peak P at 0.1 ppm has variable-temperature behavior suggestive of the other Leu 237 methyl, while the intercept for the peaks U, V, and A′ at 3.5, 3.0, and 6.0 ppm, respectively, suggests as origins the two H_β and the H_α of the same Leu 237.

Irradiation of the heme 3-CH_3 (peak b) gives significant NOEs at 5.55 (u) and 6.3 ppm (s) among others (Figure 8F). Variable-temperature data (Figure 6) show that the shifts have intercepts on the low-field side of the observed position, which dictates that they originate from an aromatic side chain which can be attributed to Phe 41. Other NOEs to peaks in the aliphatic region do not yield characteristic shifts that lead to unique assignment of amino acid residues and must await interpretation unitl an X-ray structure of HRP becomes available.

Other Resolved Non-Heme Resonances. The components of the partially resolved composite peak j, k exhibit T_1 values of ~1 s and display less than the actual one-proton intensity per component because of partial saturation at the pulse repetition rate utilized for optimal detection of all other resonances. Irradiation of peak j, k yields NOEs at 3.65 and 9.2 ppm (not shown). Neither peaks j, k nor the NOE-connected resonances exhibit temperature-dependent shifts, which, together with the long relaxation times, indicate diamagnetic residues far from the heme cavity. The apparent methyl peak, M, exhibits weak temperature dependence, with intercept at $T^{-1} = 0$ at 0.8 ppm, indicating that it arises from some aliphatic side chain in the heme pocket. Its location at –0.7 ppm places it too close to the diamagnetic envelope to allow selective irradiation. The upfield dipolar shift suggests[15,47] it arises from some unknown residue in contact with either pyrrole I or III.

Heme Orientation in Reconstituted HRP. The patterns of assigned heme methyl resonances for native HRPCN (Figure 1, R = vinyl) and deuterohemin-HRPCN (Figure 1, R = H) have indicated[37] that the respective hemes differ in orientation within the heme pocket by a 180° rotation about the α,γ-meso axis (Figure 1A,B). The location above of specific amino acid side chain signals in HRPCN now allows us to provide a more quantitative proof of this structural difference between the native and reconstituted protein. The 500-MHz ^{1}H NMR spectrum of deuterohemin-HRPCN at 55 °C in ^2H_2O is illustrated in Figure 9A. Earlier isotope labeling[37,51] identified the 1-CH_3 (b) and 5-CH_3 (a) peaks and the two-proton propionate H_β signal (peak H); peaks A and d have been assigned[42] to the proximal His 170 2′-H and 4′-H, respectively, on the basis of differential relaxation and the electronic purturbations of the heme periphery. The deuterohemin 2-H and 4-H signals were assigned on the basis of replacement, one at a time, of vinyl groups by hydrogens.[52] It has already been noted[42] that the apparent non-heme resonances exhibit essentially the same resonance positions and line widths in HRPCN and deuterohemin-HRPCN; hence the lettering scheme for resonances is selected so as to maintain the identity of amino acid peaks.

Initially, we must focus on the assignment of the remaining protons of the prosthetic group in deuterohemin-HRPCN. Saturation of 5-CH_3 yields on NOE to peak f (Figure 9B), confirming an earlier 6-H_α assignment based on titration behavior.[51] Irradiating f leads to a large NOE to its geminal partner at 10.4 ppm (peak l) as well as to 5-CH_3 (Figure 9C). Since no NOE is observed from 6-H_α to either propionate H_β in peak H, the latter peak must originate from the two 7-H_βs. Saturating 1-CH_3 yields the expected NOE to peak B, confirming its assignment to 2-H. Thus all of the resolved prosthetic group resonances in deuterohemin-HRPCN are assigned. Saturation of His 170 4′-H signal d shows an NOE to peak m at 8.4 ppm (Figure 9E). An NOE is also observed to m when peaks c and g, the His 170 H_βs, are saturated (not shown). This peak m is assigned to the H_α of His 170 on the basis of the unique proximity of this proton to 4′-H in CcP[20] and supports our assignment of the similarly located peak m to H_α in native HRPCN (see above).

Analysis of NOEs from heme functional groups to amino acid side chains reveals that 5-CH_3 (a) yields an NOE to methyl peak F (Figure 9B). Similarly, the His 170 2′-H signal, A, yields an

(51) de Ropp, J. S. Ph.D. Thesis, University of California, Davis, 1981.
(52) La Mar, G. N.; de Ropp, J. S.; Smith, K. M.; Langry, K. C. *J. Am. Chem. Soc.* **1983**, *105*, 4576–4580.

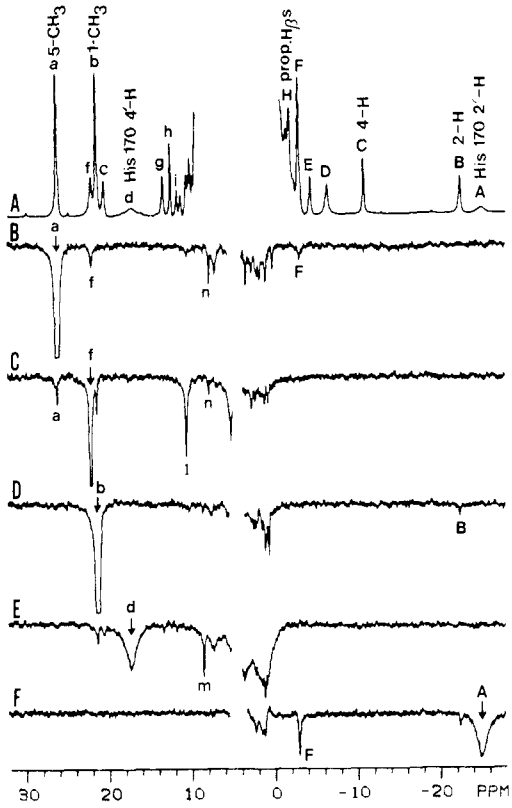

Figure 9. 500-MHz ^1H NMR spectrum of (A) 3 mM deuterohemin-HRPCN in 100% ^2H_2O at 55 °C, pH 7.0. Previously assigned[37,51] peaks are labeled. Traces B to F are the NOE difference spectra obtained upon saturating the resonance marked by an arrow. Trace B: saturate 5-CH_3; note NOEs to peak f (6-H_α) as well as peaks n and F. Trace C: saturate 6-H_α peak f; note NOEs to the geminal partner l and 5-CH_3 peak a. Also note the absence of an NOE to the propionate H_β signal H; hence H must arise from 7-H_βs. Trace D: saturate 1-CH_3; note NOE to peak B, confirming it as 2-H. Trace E: saturate His 170 4'-H signal d; note NOE to peak m. Trace F: saturation of His 170 2'-H signal A; note NOE to peak F.

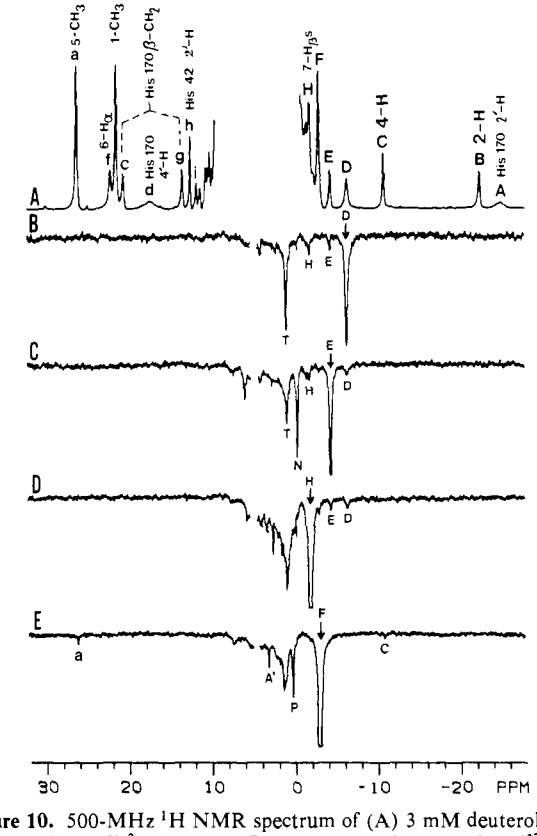

Figure 10. 500-MHz ^1H NMR spectrum of (A) 3 mM deuterohemin-HRPCN in 100% ^2H_2O at 55 °C, pH 7.0. Previously assigned[37] peaks are labeled. Traces B to E are the NOE difference spectra obtained upon saturating the resonance marked by an arrow; filled circles denote off-resonance power spillage. Trace B: saturate D; note the strong NOE to peak T and weak NOEs to E and H (7-H_βs). Trace C: saturate E; note the strong NOE to peak N and weak NOEs to D, H, and T. Trace D: saturate peak H (7-H_βs); note the reciprocal NOEs to peaks D and E. Trace E: saturate F; note the weak NOEs to 5-CH_3 (peak a) and the hemin 4-H (peak C).

NOE to F (Figure 9F). Thus peak F can be assigned to Leu 237 with the same geometrical relationship to the His 170 imidazole plane, but with contact to pyrrole III rather than IV as in native HRPCN. Saturation of the upfield peaks D and E (Figure 10B,C) yields NOE patterns essentially the same as observed for the similarly located peaks in HRPCN and confirms the same origin as Arg 38. In this case, however, we see an NOE to 7-H_β (peak H), confirming the interchange of pyrroles III and IV as compared to native HRPCN. Irradiation of 7-H_β resonance H (Figure 10D) also displays the reciprocal weak NOEs to peaks D and E. Moreover, saturating peak F (Figure 10E) yields a weak NOE to peak C as well as peak as (5-CH_3). The nearly identical dipolar shifts for the assigned amino acid peaks (Table I) of HRPCN and deuterohemin-HRPCN, together with the systematic interchange of contacts from these amino acid side chains between pyrroles I and II or III and IV, establishes that the two proteins possess essentially indistinguishable polypeptide conformation with heme orientations that differ by a 180° rotation about the α,γ-meso axis,[37] as depicted in Figure 1.

Substrate Binding Site. The ^1H NMR spectrum of HRPCN at 55 °C in the presence of 1.6 equiv of the substrate, benzhydroxamic acid (BHA), is illustrated in Figure 11A. Although there is very strong binding of BHA to HRPCN,[53] so that the binding site is saturated with only a small excess of BHA, exchange of BHA is rapid compared to the shifts induced in the complex, such that peak assignment in the HRPCN:BHA complex can be readily obtained by following peak positions during a BHA titration of HRPCN. Saturation of 8-CH_3 in a solution containing progressively less BHA is indicated in Figure 11C (0.8 equiv) and Figure 11D (0.4 equiv), with the trace obtained in the absence of BHA reproduced in Figure 11E. It can be seen that the intensity and position of peak n at 7.75 ppm are essentially independent of the amount of BHA present; the peaks at 7.6 and 7.9 ppm (designated by asterisks), on the other hand, increase in intensity as BHA is added. Thus the peak at 7.75 ppm has the same identity in substrate-free HRPCN and the 1:1 HRPCN:BHA complex, namely Tyr 185. The new peak at 7.6 and 7.9 ppm can be attributed to the bound BHA, confirming earlier suggestions[19] that the BHA binding site is near pyrrole IV. This is further supported by the fact that BHA binding purturbs the hyperfine shifts of particularly the 8-CH_3 peak and the δ-CH_3 of Leu 237 (peak F). At larger excess of BHA, the averaged BHA resonances exhibit large transferred NOE effects, as previously demonstrated for resting state HRP.[21] However, since the aromatic peak n at 7.75 ppm yields an NOE of comparable magnitude in substrate-free and substrate-bound HRPCN, the Tyr 185 in contact with the heme is not disrupted by substrate binding, as previously suggested.[21]

Discussion

Amino Acid Assignments. The assignment of amino acid resonances that are resolved and allow for the determination of NOE connectivities (or the absence thereof) among protons on the same residue can be considered definitive. Thus the presence of an arginine residue over pyrrole III is established, and the location of a distal histidine near the fourfold axis is indicated. The fact that the resonance positions of these residues are shifted precisely in the direction predicted by the known axial and rhombic magnetic anisotropy as determined previously[15] from the meso-H dipolar shift pattern supports the utility of the detailed magnetic properties of the heme in locating amino acid side chains in the

(53) Morishima, I.; Ogawa, S. *J. Biol. Chem.* **1979**, *254*, 2814–2820.

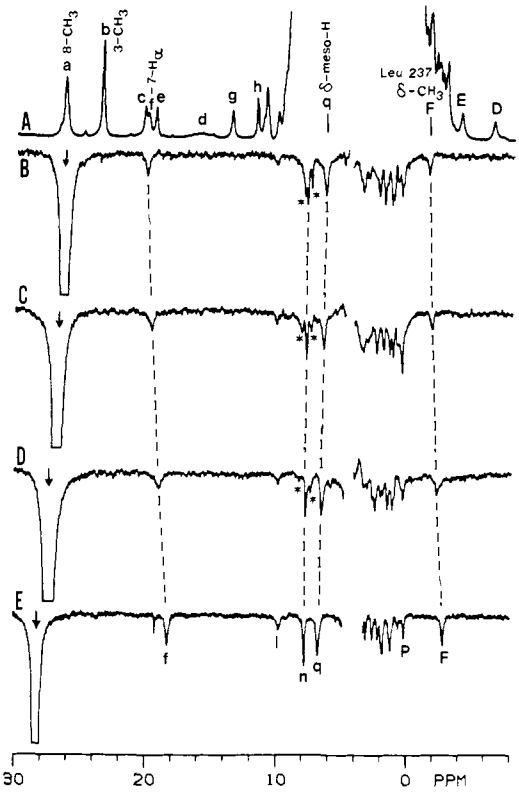

Figure 11. 500-MHz ^1H NMR spectrum of (A) 3 mM HRPCN in the presence of 1.6 equiv of benzhydroxamic acid (BHA) in 100% ^2H_2O at 55 °C, pH 7.0. Previously assigned[10,15,51] peaks are labeled. In all the difference spectra B to E, the 8-CH_3 resonance is saturated as indicated by a downward arrow. The difference spectra are obtained in the presence of the following equivalents of BHA: (B) 1.6, (C) 0.8, (D) 0.4, (E) 0.0. Note peak n (Tyr 185) remains the same in all traces while peaks f (7-H_α), q (δ-meso-H), and F (Leu 237 δ-CH_3) are shifted as the BHA concentration is increased. Also note the appearance of new peaks marked by asterisks (*) as the BHA concentration is increased; these arise from the bound BHA, as they continue to increase in intensity as more BHA is added.

heme cavity. An axial histidine with stereochemistry essentially identical with that in *Cc*P[20] is also confirmed. The identity of amino acid side chains residues in close contact with the heme which do not yield resolved resonances can, at least in principle, be identified as aromatic or nonaromatic by the intercepts in the Curie plot. Thus, while the large NOEs to peaks with intercepts below 6 ppm establish a close contact with an aromatic ring, the identity of the ring (Phe 41, Tyr 185) can only be inferred on the basis of the computer modeling and amino acid homology.[16-21]

The ability to detect numerous large and specific NOEs in such a large enzyme confirms our earlier conclusion[15] that the paramagnetic relaxation serves to essentially short circuit spin diffusion[54] without significantly decreasing the information content of the primary NOEs. For the geminal methylene group of the proximal histidine, we confirm that quantitative NOE measurements lead to useful distance information. Thus we conclude that NOE measurements, particularly in conjunction with analysis of differential relaxation, determination of the rhombic axis system from the meso-H shift pattern,[15] and the use of the Curie plot intercepts, should allow one to effectively pursue such assignment and structure determination in much larger paramagnetic enzymes. Indeed, preliminary studies indicate that largely primary and specific NOEs up to 80% are detectable between resolved resonances in the cyano complex of lactoperoxidase ($M_r \sim 78$ kD).[55]

Homology between HRP and *Cc*P. Detailed isotope labeling of the heme methyl resonances in both HRPCN[10,37] and *Cc*PCN[49] has already shown that the heme orientation relative to that of the axial histidyl imidazole is the same, namely that established by X-ray for *Cc*P[20] (trace A in Figure 1). The NOE connectivities for the remaining His 170 protons indicate a very similar geometry for the remainder of the His side chain. The location of Arg 38 over pyrrole III at a distance from the iron consistent with that residue in *Cc*P, together with the unique 2′-H proton located for the distal His 42, provides the proposed essential catalytic residues in the same sites as found in *Cc*P.[19,20] Moreover, while similar NOE studies on *Cc*P have not yet been reported, the presence of similar resonances in the low-spin cyano complexes of both proteins further supports the similarity of the stereochemistry of the heme pocket.

It appears reasonable at this time to extend such NOE studies to the wide variety of isozymes of HRP[56] or turnip peroxidase,[57] which yield distinct but very similar patterns for the hyperfine shifted resonances in the cyano complexes. Establishing similar NOE patterns as observed in HRPCN among similarly shifted resonances will confirm the presence of the same residues, and measurements of differential relaxation rates as compared to a heme methyl or differential dipolar shifts may shed light on the structural basis for varying activity among the members of a family of isozymes. The key resonances assigned to the axial His 170 (peaks d, A, c, and g), the distal His 42 (narrow peak h), and Arg 38 (peaks D and E) appear conserved in the, as yet unassigned, NMR spectra of HRPCN isozymes,[56] although with variable shifts.

Substrate Binding. ^1H NMR studies of BHA binding to resting state HRP have indicated[21] that when the accidentally degenerate 8-CH_3 and 1-CH_3 peaks are saturated, a large transferred NOE is observed for the unbound BHA in rapid exchange with bound BHA. This result was interpreted as indicating that the substrate binding site is near 8-CH_3. The selective saturation of the resolved 8-CH_3 peak in this study confirms this conclusion. The fact that the assigned Leu 237 as well as 8-CH and 7-H_α peaks are strongly perturbed upon BHA binding suggests that Leu 237 moves to accommodate BHA, and possibly also interacts with BHA. The Leu 237 δ-CH_3 peak is too close to the diamagnetic envelope to significantly saturate, so that direct transferred NOE to BHA from peak F could not be demonstrated. It has been suggested[21] that Tyr 185 is in a flexible region of the HRP polypeptide chain and that this side chain ring moves away from its contact with pyrrole IV upon BHA binding. Our observation of a strong NOE from 8-CH_3 to aromatic protons supports the presence of Tyr 185 at this position, but the presence of the unaltered NOE in the substrate-bound form dictates that it is not displaced by substrate. Thus the tools are available for studying potentially different substrate interaction with the various HRP isozymes.[56]

Heme Orientation. NOE connectivities between heme and amino acid side chains do not provide an independent determination of the absolute orientation of the heme relative to the axial His imidazole plane, as reported for Mb,[58] because of the lack of a crystal structure. However, the demonstration that the unambiguously identified amino acid residue that gives rise to peaks D and E in each of native HRPCN and deuterohemin-HRPCN interacts with pyrroles III and IV, respectively, provides a clear structural basis for assigning two different heme orientations differing by a 180° rotation about the α,γ-meso axis. This independent structural confirmation further supports the model[37,59] in which the contact shift pattern of assigned heme methyl peaks can be used to infer the absolute orientation of the heme relative to the imidazole plane in structurally uncharacterized hemoproteins.

NOE and relaxation studies of HRPCN in H_2O provide little new information on the identity of amino acid residues in the heme pocket, but they shed light on some novel aspects of the hydrogen

(54) Kalk, A.; Berendsen, J. J. C. *J. Magn. Reson.* **1976**, *24*, 343-366.
(55) Thanabal, V.; La Mar, G. N., unpublished results.
(56) Gonzalez-Vergara, E.; Meyer, M.; Goff, H. M. *Biochemistry* **1985**, *24*, 6561-6567.
(57) Williams, R. J. P.; Wright, P. E.; Mazza, G.; Ricard, J. R. *Biochim. Biophys. Acta* **1975**, *581*, 127-147.
(58) Lecomte, J. T. J.; Johnson, R. D.; La Mar, G. N. *Biochim. Biophys. Acta* **1985**, *829*, 268-274.
(59) La Mar, G. N.; Budd, D. L.; Viscio, D. B.; Smith, K. M.; Langry, K. C. *Proc. Acad. Sci. U.S.A.* **1978**, *75*, 5755-5759.

bonding network in both the proximal and distal pocket. These studies will be reported in the near future.

Acknowledgment. The authors are indebted to J. D. Satterlee for helpful discussions. This research was supported by a grant from the National Institutes of Health (GM 26226). The use of the facility of the University of California—San Francisco Computer Graphics Laboratory is gratefully acknowledged.

Registry No. CcP, 9029-53-2; L-His, 71-00-1; L-Leu, 61-90-5; L-Tyr, 60-18-4; L-Arg, 74-79-3; L-Phe, 63-91-2; heme, 14875-96-8; peroxidase, 9003-99-0.

Communications to the Editor

Measurement of ^1H-^{31}P NMR Coupling Constants in Double-Stranded DNA Fragments

Vladimír Sklenář† and Ad Bax*

Laboratory of Chemical Physics, National Institute of Diabetes and Digestive and Kidney Diseases National Institutes of Health Bethesda, Maryland 20892

Received June 15, 1987

NMR presents a unique tool for obtaining detailed conformational information about DNA fragments in solution. So far, most studies have relied on measurements of NOE buildup rates and of ^1H-^1H coupling constants.[1] Here, a new method is proposed that permits measurement of previously unresolvable $^3J_{HCOP}$ couplings, providing additional structural information about the DNA backbone. A Karplus relationship correlating $^3J_{HCOP}$ with the H–C–O–P dihedral angle has been proposed by Lankhorst et al.:[2]

$$J_{HCOP} = 15.3 \cos^2 \phi - 6.1 \cos \phi + 1.6 \qquad (1)$$

Because of the complexity of both the ^{31}P and C3′H, C5′H′, and C5′H″ multiplet structures, measurements of the J_{HP} couplings in DNA have been limited to small fragments with very narrow line widths. It is demonstrated here that for larger fragments it is also possible to measure the J_{HCOP} couplings, provided all other multiplet splittings are suppressed.

Homonuclear couplings to the C3′H resonance can be removed in a 2D experiment by the application of a selective 180° refocusing pulse in the middle of the evolution period, affecting only the C3′ protons. Since the C3′H resonances in DNA usually are separated from the C4′ and C2′ protons, such an experiment presents no particular difficulty. Two possible schemes incorporating this idea are

$$\begin{array}{ll} ^1H: & 90_x\text{–}t_1/2\text{–}90_{\phi,sel}\text{–} \quad 180° \quad \text{–}90_{\phi,sel}\text{–}t_1/2\text{–acq } (\psi) \\ ^{31}P: & \qquad\qquad\qquad\qquad \text{decouple} \end{array} \qquad (A)$$

$$\begin{array}{ll} ^1H: & \text{presaturate–} \quad -180_{x,sel}\text{–}180_x\text{–} \quad \text{–}90_x\text{–acq } (\psi) \\ ^{31}P: & \qquad 90_\phi\text{–}t_1/2 \qquad\quad t_1/2\text{–}90_x \end{array} \qquad (B)$$

Scheme A is a variation on the heteronuclear proton-flip experiment;[3] scheme B is a selective version of the ^1H-detected heteronuclear correlation scheme.[4] The phase cycling for A is $\phi = x, y, -x, -y$ and $\psi = +, -, +, -$. For scheme B, $\phi = x, y, -x, -y$ and $\psi = +, +, -, -$, with data acquired in odd- and even-numbered scans being stored separately and processed to yield 2D absorption mode spectra.[5] For the selective pulses, we use low-power rectangular shapes although better results may be obtainable with shaped pulses. Since the C3′H region to be inverted is often quite close to some of the C4′H resonances, optimal setting of the selective pulse duration and rf power is important. If the C3′H region to be inverted covers a spectral width of N Hz, we recommend using an rf field strength of about N Hz with the carrier positioned in the center of the C3′H region. For scheme A, the J_{PH} coupling appears in the F_1 dimension and the resolution in this direction is determined by the ^1H T_2 value. For scheme B, all but the $J_{P\text{–}C3'H}$ couplings have been removed in the F_1 (^{31}P) dimension of the 2D correlation map. ^{31}P T_2 values are the limiting factor for resolution in this dimension.

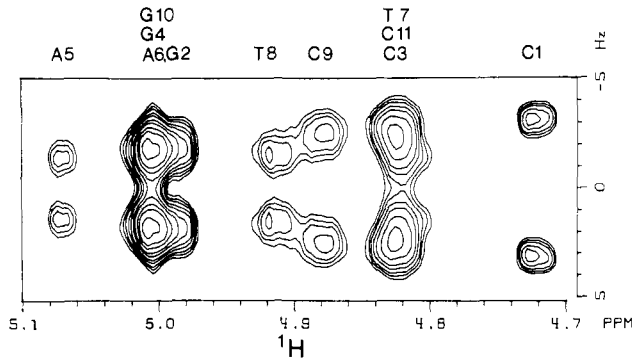

Figure 1. ^1H-detected 500-MHz 2D J spectrum of d-(CGCGAATTCGCG)$_2$ recorded with scheme A. The C3′H chemical shifts appear along the horizontal axis, with the corresponding $^3J_{HP}$ couplings along the vertical axis. An exponential line narrowing of 1.5 Hz has been used in the F_1 dimension.

The utility of these two methods is illustrated by applying them to a sample of the dodecamer d(CGCGAATTCGCG)$_2$ in D_2O, p^{2}H 7, 100 mM NaCl, 36 °C. Figure 1 presents a 2D J spectrum recorded with scheme A at 500 MHz. The indicated assignments of the C3′H resonances were obtained from a NOESY spectrum and are in agreement with results presented by Hare et al.,[6] except for very small changes in chemical shifts due to slightly different conditions. Only four of the C3′H resonances are resolved sufficiently to yield reliable coupling constants. Approximate values can be obtained for the partially resolved resonances of the G2 and T7 nucleotides. The nearly complete overlap of the C3′H resonances of A6/G4/G10 and C11/C3 prevents measurement of the corresponding couplings. This overlap of the ^1H resonances is removed in the correlation spectrum (Figure 2) recorded with scheme B. Because ^{31}P relaxation is dominated by chemical shift anisotropy, a considerable lengthening (by a factor of 2) of the ^{31}P T_2 was obtained by recording this spectrum at 270 MHz instead of 500 MHz. The expected loss in F_1 resolution due to the smaller chemical shift dispersion at this lower field is largely offset by the longer ^{31}P T_2 and more importantly by the decrease in the F_1 multiplet width caused by the partial decoupling provided

†On leave from the Institute of Scientific Instruments, Czechoslovak Academy of Sciences, CS 61264 Brno, Czechoslovakia.

(1) Wuthrich, K. *NMR of Proteins and Nucleic Acids*; Wiley: New York, 1986; Chapter 13.
(2) Lankhorst, P. P.; Haasnoot, C. A. G.; Erkelens, C.; Altona, C. *J. Biomol. Struct. Dyn.* **1984**, *1*, 1387.
(3) Bax, A.; Freeman, R. *J. Am. Chem. Soc.* **1982**, *104*, 1099.
(4) Sklenář, V.; Miyashiro, H.; Zon, G.; Miles, H. T.; Bax, A. *FEBS Lett.* **1986**, *208*, 94.
(5) States, D. J.; Haberkorn, R. A.; Ruben, D. J. *J. Magn. Reson.* **1982**, *48*, 286.
(6) Hare, D. R.; Wemmer, D. E.; Chou, S. H.; Drobny, G.; Reid, B. R. *J. Mol. Biol.* **1983**, *171*, 319.

This article not subject to U.S. Copyright. Published 1987 by the American Chemical Society